Influence of radiation heat transfer on parallel hot-wire thermal conductivity measurements of semi-transparent materials at high temperature

Léa Penazzi, Yves Jannot, Johann Meulemans, Olivier Farges, Vincent Schick

Influence of radiation heat transfer on parallel hot-wire thermal conductivity measurements of semi-transparent materials at high temperature

Léa Penazzi[a,b], Yves Jannot[a,b], Johann Meulemans[b,c], Olivier Farges[a,b], Vincent Schick[a,b]

[a] *Université de Lorraine, CNRS, LEMTA, F-54500 Vandœuvre-lès-Nancy, France*
[b] *Laboratoire Commun Canopée, CNRS, Université de Lorraine, Saint-Gobain*
[c] *Saint-Gobain Research Paris, 39 quai Lucien Lefranc, F-93303 Aubervilliers, France*

Abstract

This paper presents a study of the influence of the radiation transfer on the thermal conductivity measurement in a parallel hot-wire method at high temperature. Simulations of the temperature evolution are first carried out with COMSOL Multiphysics® using the coupled conduction-radiation module based on the P1 approximation for the radiation calculation. A wide range of conditions were investigated: a low and a high density insulator were considered with various radiation characteristics (purely scattering, absorbing and scattering, purely absorbing) and with temperature varying up to 1500 °C. This study enables the determination of the validity limit of the modeling of the temperature by a purely conductive model with an equivalent conductivity based on the Rosseland approximation. When this assumption is valid, a new estimation process was proposed to improve the estimation accuracy of the thermal properties. A calibration process of the distance between the hot-wire and the thermocouple has also been proposed and validated, enabling a more accurate estimation of the volume heat capacity.

An experimental study carried out on three insulating materials with densities ranging from $581\,\mathrm{kg \cdot m^{-3}}$ to $910\,\mathrm{kg \cdot m^{-3}}$ and at temperatures ranging from 20 °C to 1200 °C confirms the results of the theoretical study. Finally, a method enabling the estimation of the extinction coefficient from thermal conductivity measurements at various temperatures is presented and successfully applied to the three tested materials.

Keywords: Conduction ; Radiation ; Thermal conductivity ; Estimation method ; Parallel hot-wire.

1. Introduction

As previously pointed out in [1], knowledge of the thermal conductivity of high temperature insulating materials is of great importance for the control of industrial processes. It has also been stated that the parallel hot-wire method is one of the most suited method to measure the thermal conductivity at high temperature [1, 2], moreover it is a standardized method [3]. Some recent developments in the modelling of this method have led to a better accuracy of the measurement [1, 3]. Nevertheless, the estimation process is more often based on a purely conductive model, considering an equivalent thermal conductivity that is the sum of the thermal conductivity and of the radial conductivity [1, 2, 3, 4, 5, 6]. This approximation holds true for optically thick media.

Some authors investigated the effect of radiation heat transfer without making this assumption.Ebert and Fricke [7] simulated the heat transfer in a hot-wire measurement with a one dimensional coupled conduction-radiation model valid only for optically thick media. The radiation emitted by the heating wire was also neglected. Their theoretical study showed that the hot-wire method is applicable only if the extinction coefficient exceeds a critical value. Gross et al. [8] simulated the heat transfer in a hot-wire measurement with a one dimensional coupled conduction-radiation model solved by the discrete ordinates method. They showed that this critical value increases with the temperature. The influence of the proportion of diffusion/absorption in the extinction coefficient was not addressed in their theoretical study. Coquard et al. [9] developed a two dimensional coupled conduction-radiation model solved by the discrete ordinates method. They used it to

Email address: lea.penazzi@univ-lorraine.fr (Léa Penazzi)

Nomenclature

Greek Symbols

β	Extinction coefficient (m^{-1})
λ	Thermal conductivity of the considered material ($\mathrm{W} \cdot \mathrm{m}^{-1} \cdot \mathrm{K}^{-1}$)
Ω	Solid angle (sr)
ϕ	Heat flux density ($\mathrm{W} \cdot \mathrm{m}^{-2}$)
ρ	Density ok the material ($\mathrm{kg} \cdot \mathrm{m}^{-3}$)
σ	Stefan-Boltzmann constant ($\mathrm{W} \cdot \mathrm{m}^{-2} \cdot \mathrm{K}^{-4}$)
τ	Optical thickness (–)
θ	Laplace transform of $T(d,t)$
ε	Emissivity (–)
φ_w	Linear heat flux produced by the heating wire ($\mathrm{W} \cdot \mathrm{m}^{-1}$)
$\boldsymbol{\omega}$	Direction (–)

Latin Symbols

$\mathcal{I}$	Radiant intensity ($\mathrm{W} \cdot \mathrm{m}^{-2} \cdot \mathrm{sr}^{-1}$)
$\mathbf{n}$	Outward unit direction on the surface (–)
a	Thermal diffusivity of the isotropic material ($\mathrm{m}^2 \cdot \mathrm{s}^{-1}$)
c	Heat capacity of the material ($\mathrm{J} \cdot \mathrm{kg}^{-1} \cdot \mathrm{K}^{-1}$)
d	Distance between the heating wire and the thermocouple (m)
G	Incident radiation ($\mathrm{W} \cdot \mathrm{m}^{-2}$)
I	Electrical intensity passing through the heating wire (A)
k_a	Absorption coefficient (m^{-1})
k_s	Scattering coefficient (m^{-1})
K_i	Modified Bessel functions of the second kind $i \in \{0;1\}$
l_w	Length of the heating wire (m)
N	Stark number (–)
n	Refractive index (–)
P	Phase function (–)
p	Laplace parameter (s^{-1})
Q_r	Radiative heat source ($\mathrm{W} \cdot \mathrm{m}^{-3}$)
R	Thermal contact resistance between the heating wire and the sample ($\mathrm{K} \cdot \mathrm{W}^{-1}$)
r_w	Radius of the heating wire (m)
R_el	Electrical resistance of the heating wire (Ω)
T	Temperature (K)
U	Voltage at the heating wire terminals (V)

Subscripts

$_\mathrm{c}$	Relating to the conductive transfer (–)
$_\mathrm{r}$	Relating to the radiative transfer (–)
$_\mathrm{w}$	Relating to the hot wire (–)
$_\mathrm{exp}$	Relating to the experimentation (–)
$_\mathrm{mod}$	Relating to the modelling (–)

study the accuracy of the estimation of the thermal conductivity by the hot-wire method, they highlighted the estimation bias for materials of low density or low optical thickness. Nevertheless, the study was applied to only one material (an EPS foam) and at ambient temperature. Daouas et al. [10] simulated the heat transfer in a parallel hot wire measurement with a one dimensional coupled conduction-radiation model solved by the discrete ordinates method. A sensitivity study showed the possibility of estimating the absorption coefficient in addition to the thermal parameters. However, the study was performed at room temperature on a very weakly absorbing and non-scattering material.

The purpose of this study is to establish the conditions under which the temperature evolution in a parallel hot-wire measurement can be correctly represented by a pure conductive model using an apparent thermal conductivity. A theoretical study using the P1 appriximation method implemented in COMSOL Multiphysics® will be performed for temperatures ranging from ambient to 1500 °C, for both absorbing and scattering media and for several densities, extending the range of materials and temperatures of the previous studies. When the purely conductive model applies, a new estimation method is proposed that improves both thermal conductivity and thermal capacity estimations. A calibration process of the distance between the hot wire and the thermocouple will also be proposed, enabling a more accurate estimation of

the volumetric heat capacity. The results will be supported by an experimental study carried out on three insulating materials with densities ranging from $581\,\mathrm{kg}\cdot\mathrm{m}^{-3}$ to $910\,\mathrm{kg}\cdot\mathrm{m}^{-3}$ and at temperatures ranging from 20 °C to 1200 °C. Finally, a method enabling the estimation of the extinction coefficient from thermal conductivity measurements at various temperatures is presented and successfully applied to the three tested materials.

2. Principle and models

2.1. Principle

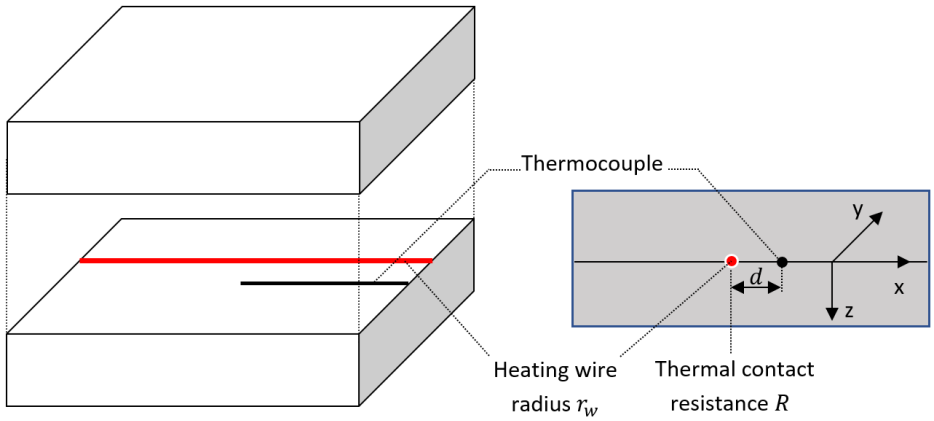

Figure 1: Schematic view of a parallel hot-wire set-up

The schematic diagram of the classical parallel hot-wire set-up is presented in Figure 1. A resistive heating wire with a radius r_w is inserted in a groove placed on the surface of the bottom sample. A thermocouple is inserted in another groove placed at the surface of the same sample at distance d of the heating wire. A second sample with the same dimensions as the bottom sample is then placed on top of it. A constant heat flow rate is then imposed in the heating wire by passing an electrical current with a constant intensity I. The equations of the system are:

$$\begin{cases} \rho c \dfrac{\partial T}{\partial r} = \boldsymbol{\nabla}\cdot(\lambda_\mathrm{c}\boldsymbol{\nabla}T) & (1)\\ T(r,0) = 0 & (2)\\ \lim\limits_{r\to\infty} T(r,0) = 0 & (3)\\ \varphi_w = \rho_\mathrm{w} c_\mathrm{w} \pi r_\mathrm{w}^2 \dfrac{\partial T_\mathrm{w}}{\partial t} + \dfrac{T_\mathrm{w} - T(r_\mathrm{w})}{R l_\mathrm{w}} & (4) \end{cases}$$

A complete model of the system can be found in [1], it is based on the following hypotheses:

- The samples are infinite in the Ox and Oz directions (semi-infinite medium hypothesis).
- There is no temperature gradient along the Oy direction ("long wire").
- The heat flow rate φ_w produced in the heating wire is constant.
- The mass of the thermocouple is negligible.
- Radiation heat transfer is negligible or may be represented by an apparent thermal conductivity.

Jannot and Degiovanni [1] established the following expression for the Laplace transform of the thermocouple temperature:

$$\theta(d,p)=\frac{\frac{\varphi_{\mathrm{w}}}{pl_{\mathrm{w}}}K_0(\sqrt{\frac{p}{a}}d)}{\rho_{\mathrm{w}}c_{\mathrm{w}}\pi r_{\mathrm{w}}^2pK_0\left(\sqrt{\frac{p}{a}}r_{\mathrm{w}}\right)+2\pi\lambda_{\mathrm{c}}\sqrt{\frac{p}{a}}r_{\mathrm{w}}\left[1+\rho_{\mathrm{w}}c_{\mathrm{w}}\pi {r_{\mathrm{w}}}^2pRl_{\mathrm{w}}\right]K_1\left(\sqrt{\frac{p}{a}}r_{\mathrm{w}}\right)} \tag{5}$$

The temperature rise $T(d,t)$ is calculated by applying an inverse Laplace transform to Equation (5) using the De Hoog algorithm [11].

2.2. General equations

It is assumed here that the medium is grey. The coupled conduction and radiation heat transfer in transient hot-wire measurements is described by the following energy balance:

$$\rho c\frac{\partial T}{\partial t}=-\boldsymbol{\nabla}\cdot(\boldsymbol{\phi}_{\mathrm{c}}+\boldsymbol{\phi}_{\mathrm{r}}) \tag{6}$$

Where $\boldsymbol{\phi}_{\mathrm{c}}$ is the conductive heat flux given by Equation (7) and $\boldsymbol{\phi}_{\mathrm{r}}$ is the radiative flux given by Equation (8).

$$\begin{cases}\phi_{\mathrm{c}}=-\lambda_{\mathrm{c}}\dfrac{\partial T}{\partial \mathrm{r}} & (7)\\ \boldsymbol{\nabla}\cdot\boldsymbol{\phi}_{\mathrm{r}}=4k_{\mathrm{a}}n^2\sigma T^4-k_{\mathrm{a}}\displaystyle\int_{4\pi}\mathcal{I}\left(\boldsymbol{\omega}\right)\mathrm{d}\Omega & (8)\end{cases}$$

$\mathcal{I}(\boldsymbol{\omega})$ is the radiant intensity in the $\boldsymbol{\omega}$ direction given by the radiative transfer equation (RTE) (Equation (9)):

$$\frac{\partial\mathcal{I}\left(\boldsymbol{\omega}\right)}{\partial s}=-\left(k_{\mathrm{a}}+k_{\mathrm{s}}\right)\mathcal{I}\left(\boldsymbol{\omega}\right)+k_{\mathrm{a}}\ n^2\sigma T^4+\frac{k_{\mathrm{s}}}{4\pi}\int_{4\pi}\mathcal{I}\left(\boldsymbol{\omega'}\right)P\left(\boldsymbol{\omega'}\rightarrow\boldsymbol{\omega}\right)\mathrm{d}\Omega' \tag{9}$$

2.3. Model M1: P1 approximation

The P1 approximation, corresponding to a spherical harmonics method (PN) truncated at the first order, enables solving the RTE presented in Equation (9). The P1 approximation relies on the assumption that the scattering is linear isotropic [12]. This assumption is justified in this present configuration as the medium is optically thick, $\tau\gg1$, where τ is the optical thickness defined by the integral of the extinction coefficient β along a typical optical path $\tau=\int_0^s\beta\mathrm{d}s$.

From a computational point of view this approximation has a limited impact because it introduces only one additional degree of freedom for the incident radiation G ($\mathrm{W}\cdot\mathrm{m}^{-2}$), which is a scalar quantity and adds a heat source or sink to the temperature equation to account for radiative heat transfer contributions. This method, however, fails to accurately represent cases where the radiative intensity propagation dominates over its diffusivity or where the scattering effects cannot be described by a linear isotropic phase function. The P1 approximation is a simplified approach, which is expected to be fairly good for absorbing and highly scattering media at large optical distances from boundaries or interfaces that have a strong variation oftemperature and radiative characteristics of the medium [12]. The P1 approximation solves the RTE equation, expressed in Equation (9), by solving the following equation:

$$\boldsymbol{\nabla}\cdot(-D_{P1}\boldsymbol{\nabla}G)=-Q_{\mathrm{r}} \tag{10}$$

Where G is the incident radiation (Equation (11)), D_{P1} is the P1 diffusion coefficient in the case of an isotropic diffusion (Equation (12)) and Q_{r} is the radiative volumetric heat source (Equation (13)).

$$\begin{cases} G = \displaystyle\int_0^{4\pi} \mathcal{I}\left(\boldsymbol{\omega}\right) \mathrm{d}\Omega & (11) \\ D_{P1} = \dfrac{1}{3k_\mathrm{a} + 3k_\mathrm{s}} & (12) \\ Q_\mathrm{r} = \boldsymbol{\nabla} \cdot \boldsymbol{\phi}_\mathrm{r} = k_\mathrm{a}(G - 4k_\mathrm{a}\ n^2\sigma T^4) & (13) \end{cases}$$

Regarding the boundary conditions, at the hot wire surface, thermocouples surfaces and sample external surfaces are considered as opaque surfaces. The following equation accounts for the radiation emitted/absorbed by the boundaries and is known as the Marshak's boundary condition [13]:

$$\mathbf{n} \cdot (-D_{P1} \boldsymbol{\nabla} G) = \phi_{\mathrm{r,net}} \tag{14}$$

Where $\phi_{\mathrm{r,net}}$ is the net radiative heat flux at the boundary and $\mathbf{n}$ the outward unit direction on the surface. In the following simulations, surfaces of the hot wire, thermocouples and the external surface of the sample were considered grey with an approximate common emissivity value of $\varepsilon = 0.8$. The net radiative heat flux is then expressed as follows:

$$\phi_{\mathrm{r,net}} = \frac{\varepsilon}{2(2-\varepsilon)}(4n^2\sigma T^4 - G) \tag{15}$$

2.4. Model M2: Rosseland approximation

If the medium is grey and optically thick, the radiative flux divergence is expressed as follows :

$$\phi_\mathrm{r} = -\lambda_\mathrm{r} \frac{\partial T}{\partial r} \tag{16}$$

With the expression of the radiative thermal conductivity [14] :

$$\lambda_\mathrm{r}(T) \ = \frac{16}{3} \ \frac{n^2\sigma\ T^3}{\beta} \tag{17}$$

where β is the extinction coefficient of the medium given by $\beta = k_\mathrm{a} + k_\mathrm{s}$. We are thus brought back to a pure conduction problem with an apparent conductivity $\lambda = \lambda_\mathrm{c} + \lambda_\mathrm{r}$.

3. Materials and experimental device

An experimental study was carried out to confirm the theoretical results. Measurements were undertaken on an isotropic material : SilPower® (Saint-Gobain) with three different densities: 581, 741 and 910kg $\cdot$ m^{-3} referenced respectively as *SG*, *MG* and *HG*. SilPower®Rigid Silica is a high performance infra-red reflector obtained from Quartzel® fibers having an SiO_2 content $\geq 99.95\,\%$ (Saint-Gobain, 2021).

The dimensions of the samples are 230 x 120 x 60 mm^3 as recommended by the standard ISO 8894-2:2007. The parallel hot-wire (PHW) measurements were conducted at 20, 200, 400, 600, 800, 1000 and 1200°C. Three experiments were carried out for each temperature and for each density. Figure 2 presents a schematic view of the measurement set-up. The heating wire made of Nickel-Chrome 80/20 has a diameter of 0.5 mm and it is inserted in a groove with a 0.5 $\times$ 0.5mm^2 section. The groove with the same length as the sample was machined in the middle of one face of the sample.

To study the influence of the distance between the heating wire and the thermocouple, the temperature rise was measured at two locations, respectively at $d_1 \approx$10 mm and $d_2 \approx$15 mm from the heating wire. The temperature measurements were carried out with two type N sheath thermocouples with an outer diameter of 0.5 mm, inserted in grooves with a 0.5 $\times$ 0.5mm^2 section machined on the half-length of the sample in

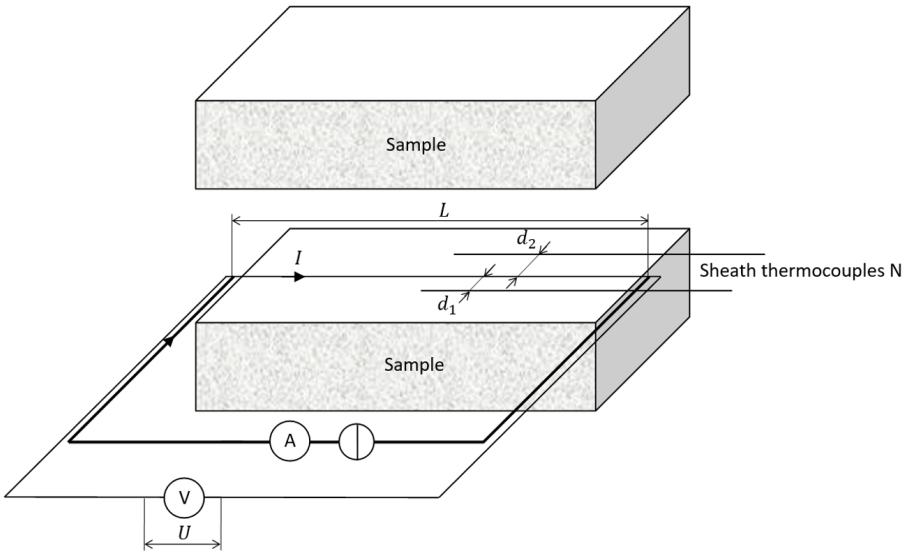

Figure 2: Schematic view of the measurement set-up.

order to measure the temperature at the center. The temperature is recorded with 0.1 s time step by a data logger Picolog TC08. The standard deviation of the temperature measurement is 0.01 °C before heating.

The device was placed in an electric fusing kiln (Vecstar furnace) equipped with a temperature controller (Watlow EZ-Zone) ensuring a very good temperature stability inside the kiln (±1 °C).

Two wires were point-welded on the heating wire with a distance $l_w = 235\,\text{mm}$ between the two weldings (see Figure 2). These wires were connected to a voltmeter (Almemo 2890-9) to measure the electrical voltage U between the two points. A stabilized power supply (Tektronix PWS2185) produces an electrical current with a constant intensity I passing through the wire. These measurements allow the calculation of the electrical resistance per meter of the heating wire with the following formula:

$$\frac{R_{el}}{l_w} = \frac{U}{I l_w} \tag{18}$$

4. Estimation method

In previous works [1, 3], the Levenberg-Marquart algorithm [15] was used to find the values of the unknown parameters λ, ρc and R that minimize the sum of the quadratic errors:

$$S = \sum_{n=1}^{N} \left[T_{exp}(d,t) - T_{mod}(d,t)\right]^2 \tag{19}$$

Where T_{mod} is calculated by inverse Laplace transform of Equation (5). Using this estimation method, it was found that the estimated values of decrease and become negative when the temperature increases which does not make any physical sense. As an example, Figure 3a represents: the experimental curve and the model curve plotted with the triplet $(\lambda, \rho c, R)$ of the estimated values, the model curve plotted with the triplet $(\lambda, \rho c, R = 0)$ as well as the residuals (multiplied by 10 for a better reading) for an experiment on the SilPower®SG at 600 °C for which the estimation over the interval $[100\,\text{s}, 900\,\text{s}]$ led to the value $R = -5.8\,\text{K}\cdot\text{W}^{-1}$. It can be seen that the estimation residuals are perfectly flat over the estimation interval which means that from 100 s onwards, the Rosseland assumption is verified, hence, in this case, the use of the model is validated. Between 0 s and 100 s (see Figure 3b), the experimental temperature is higher than the model temperature which means that the heat flux transmitted by radiation is higher than that predicted

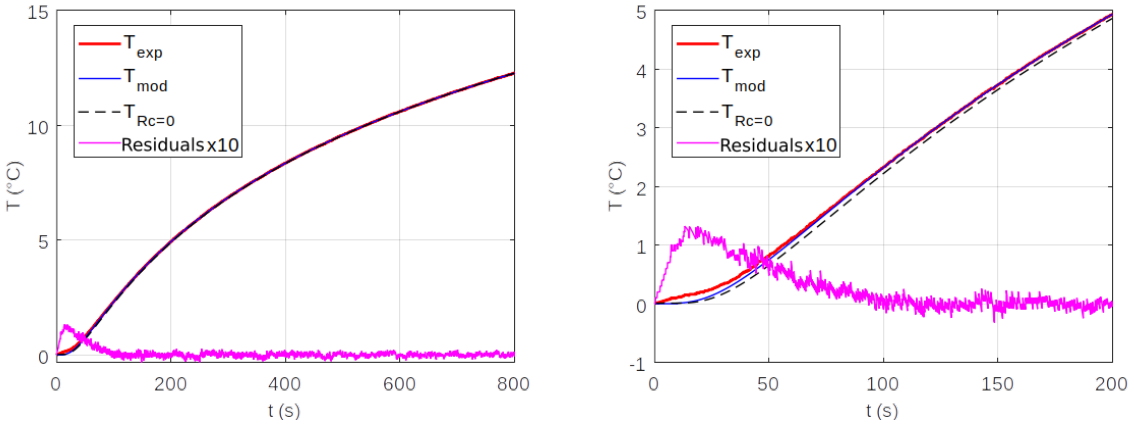

(a) From 0 s to 800 s

(b) From 0 s to 200 s

Figure 3: Experimental and simulated curves with estimation residuals ×10 for an experiment with SilPower®SG at 600 °C.

by the model. The negative value of the contact resistance compensates for this model bias and thus has the effect of shifting the temperature so that is obtained $T_{\text{exp}}(100\,\text{s}) = T_{\text{mod}}(100\,\text{s})$.

However, it has another undesirable effect illustrated in Figure 4, which depicts the reduced temperature sensitivity to the contact resistance for different values of the contact resistance. The value $R = 2\,\text{K}\cdot\text{W}^{-1}$ is an average value consistent with those obtained from COMSOL Multiphysics® simulations of our device. We can see that the sensitivity to R which varies little with the value $R = 2\,\text{K}\cdot\text{W}^{-1}$ varies significantly for strongly negative values of R. We will show that this can create an estimation bias on the values of λ and ρc.

To do so, we performed a simulation based on Equation (5) with the estimated values $\lambda = 0.22\,\text{W}\cdot\text{m}^{-1}\cdot\text{K}^{-1}$ and $\rho c = 6.11\times10^{5}\,\text{J}\cdot\text{m}^{-3}\cdot\text{K}^{-1}$ and considering $R = 2\,\text{K}\cdot\text{W}^{-1}$, and then we added to the result a constant value T_0. This T_0 value thus represents the contribution of radiation between 0 and 100 s not taken into account by the Rosseland model.

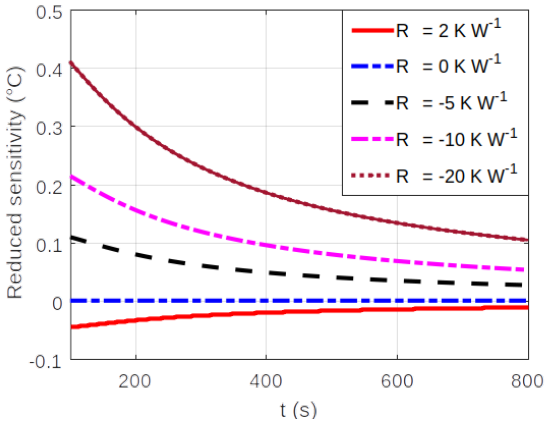

Figure 4: Reduced sensitivity of the temperature according to thermal contact resistance R values ($\lambda = 0.22\,\text{W}\cdot\text{m}^{-1}\cdot\text{K}^{-1}$; $\rho c = 6.11\times10^{5}\,\text{J}\cdot\text{m}^{-3}\cdot\text{K}^{-1}$).

Two estimation methods were then applied to this curve over the interval $[100\,\text{s}, 800\,\text{s}]$:

- An estimation E1 of $(\lambda, \rho c, R)$ as described above.
- An estimation E2 of $(\lambda, \rho c, T_1)$ by calculating the temperature from the Equation (5), considering

$R = 0\,\mathrm{K}\cdot\mathrm{W}^{-1}$ and adding a constant value T_1 that is:

$$T(d,t) = \mathcal{L}^{-1}\left[\frac{\frac{\varphi_\mathrm{w}}{pL}K_0\left(\frac{p}{a}d\right)}{\rho_\mathrm{w}c_\mathrm{w}\pi {r_\mathrm{w}}^2 pK_0\left(\frac{p}{a}r_\mathrm{w}\right) + 2\pi\lambda\frac{p}{a}r_\mathrm{w}K_1\left(r\frac{p}{a_\mathrm{w}}\right)}\right] + T_1 \tag{20}$$

Where $\mathcal{L}^{-1}$ is the operator of the inverse Laplace transform. Table 1 shows the estimation results for different values of T_0. It can be observed that the E2 estimation method leads to a constant error of 0.7 % on λ and a negligible error on ρc. The E1 method leads to a small estimation error on λ (less than 1 % if $T_0 < 0.75\,°\mathrm{C}$) but a large error on ρc that increases with T_0. We therefore treated the experimental curves using the E2 estimation method and choosing an estimation interval such that the residuals are flat and centered on zero over this interval.

Table 1: Estimated values of the parameters by the two methods E1 and E2 for different values of the temperature step due to radiation between 0 s to 100 s with $\lambda = 0.22\,\mathrm{W\ m^{-1}\ K^{-1}}$, $\rho c = 6.11\times10^5\,\mathrm{J\ m^{-3}\ K^{-1}}$.

	$\mathbf{T_0}$	°C	**0**	**0.25**	**0.5**	**0.75**	**1.0**	**1.25**	**1.5**
E1	λ	$\mathrm{W\ m^{-1}\ K^{-1}}$	0.22	0.2192	0.2194	0.2177	0.2171	0.2165	0.2159
	ρc	$\mathrm{J\ m^{-3}\ K^{-1}}$	6.11	5.914	5.724	5.554	5.358	5.183	5.014
	R	$\mathrm{K\ W^{-1}}$	2.0	-4.0	-9.8	-15.4	-20.8	-26.0	-31.3
E2	λ	$\mathrm{W\ m^{-1}\ K^{-1}}$				0.2185			
	ρc	$\mathrm{J\ m^{-3}\ K^{-1}}$				6.112			
	T_1	°C	-0.019	0.231	0.481	0.731	0.981	1.231	1.481

5. Validity of the Rosseland model

To determine the validity limits of Rosseland model in the case of the parallel hot-wire method, we performed simulations using the COMSOL Multiphysics® coupled conduction-radiation transfer solver based on the approximate model P1 [16].

Conduction is modeled with the energy balance equation with a radiative source term (Equations (6) to (8)). The radiative source term is modeled with the P1 approximation (Equations (10) to (15)). The solution of the transient coupled conduction and radiation equations is solved iteratively by the Finite Element method (FEM). Solid domains formed by the hot wire, the two thermocouples and the sample are meshed with 4974 unstructured tetrahedrals. The maximum size of an element size is 6.36×10^{-3} m and the minimum size of an element is 3.6×10^{-5} m. The mesh is automatically created and adapted for the model's physics settings. The time dependency in the FEM is solved by an implicit BDF (Backward Differentiation Formula) method. This implicit solver uses an backward differentiation formulas with order of accuracy varying from one (also known as the backward Euler method) to two. The time step used for the simulation is 0.1 s.

We first compared the solutions given by COMSOL Multiphysics® with the exact solution in two asymptotic cases where an analytical solution exists as proposed by Gross et al. [8]:

- The case where the extinction coefficient is very large ($k_\mathrm{a} = k_\mathrm{s} = 1\times10^8\,\mathrm{m^{-1}}$), the temperature evolves as in the case of a purely conductive transfer because $\lambda_\mathrm{r} = 0\,\mathrm{W\cdot m^{-1}\cdot K^{-1}}$.
- The case where the material is completely transparent ($k_\mathrm{a} = k_\mathrm{s} = 0\,\mathrm{m^{-1}}$) with perfectly reflecting surfaces, the transfer is also purely conductive (zero radiation).

The geometry considered is a cylinder with an external diameter of 50 mm heated uniformly on its internal diameter of 0.5 mm, both surfaces being opaque and insulated, and the initial uniform temperature being equal to 1000 °C.

As an example, Figure 5a represents for the case of the transparent material the curves of the temperature at a distance $d = 15$ mm from the heating wire, obtained with COMSOL Multiphysics®on the one hand

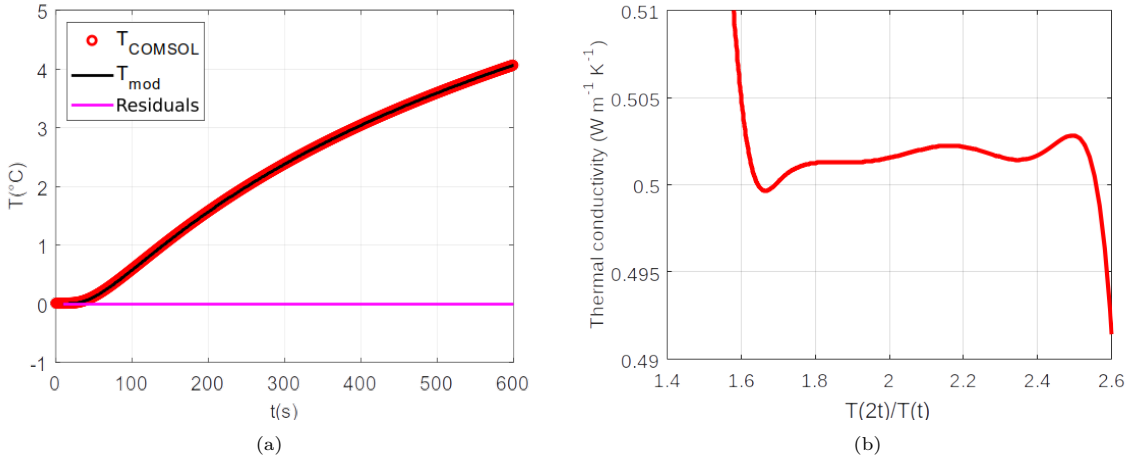

(a) (b)

Figure 5: (a) - Temperature curves simulated with COMSOL Multiphysics® and with the exact analytical model ($\lambda_c = 0.5\,\mathrm{W\cdot m^{-1}\cdot K^{-1}}$; $k_a = k_s = 0\,\mathrm{m^{-1}}$) ; (b) - Estimated values of λ by processing the COMSOL Multiphysics®curve with the standard method ISO 8894-2:2007.

and with the exact analytical model on the other hand for the following values of the parameters: $\lambda_c = 0.5\,\mathrm{W\cdot m^{-1}\cdot K^{-1}}$, $\rho c = 10^6\,\mathrm{J\cdot m^{-3}\cdot K^{-1}}$. The curves are in very good agreement and estimates made from the curves simulated with COMSOL Multiphysics®using the ISO 8894-2:2007 method [2] lead to values of λ that differ by less than 0.5 % from the nominal value as shown in fig. 5b. The ISO 8894-2:2007 method [2] was detailed in a previous paper [1], it recommends the estimation for values of the ratio $T(2t)/T(t)$ between 1.5 and 2.4, in the presented case the validity limit of the semi-infinite medium assumption reduces this interval to $[1.7, 2.4]$. The results obtained in the case where the extinction coefficient is very large are similar.

After this validation phase, we performed simulations with COMSOL Multiphysics®of the experimental setup shown in Figure 6. For each simulation, the temperatures of the heating wire and of the two thermocouples placed respectively at 10 mm and 15 mm from the heating wire were recorded.

Preliminary tests were carried out in order to ensure the simulations results independence to temporal and spatial discretizating. The simulations were performed between 0 s to 1000 s:

- For two temperatures: 1000 °C and 1500 °C.
- For two typical materials: a low density thermal insulating material ($\lambda_c = 0.1\,\mathrm{W\cdot m^{-1}\cdot K^{-1}}$ and $\rho c = 2.5\times10^5\,\mathrm{J\cdot m^{-3}\cdot K^{-1}}$) and a high density thermal insulating material ($\lambda_c = 0.5\,\mathrm{W\cdot m^{-1}\cdot K^{-1}}$ and $\rho c = 10^6\,\mathrm{J\cdot m^{-3}\cdot K^{-1}}$).
- For four values of the extinction coefficient β, *ie* $500\,\mathrm{m^{-1}}$, $1000\,\mathrm{m^{-1}}$, $5000\,\mathrm{m^{-1}}$ and $10\,000\,\mathrm{m^{-1}}$ and for each value of β the following three values of k_a were considered: $k_a = 0.0001\times\beta; 0.5\times\beta; \beta$ (with $k_s = \beta - k_a$). The extreme cases correspond respectively to pure scattering and pure absorption.

The absorption coefficient was not chosen equal to zero because it has been shown [17] that in this case the radiative transfer could be represented by a parallel resistance between the two surfaces, which would invalidate the semi-infinite medium hypothesis even at short times. We chose a minimum value equal to $0.0001\times\beta$.

The refractive index of the medium was chosen equal to unity and the emissivities of the wire and of the thermocouples equal to 0.8. The thermal properties of the heating wire and thermocouple are those of a stainless steel: $\lambda = 11\,\mathrm{W\cdot m^{-1}\cdot K^{-1}}$ and $\rho c = 3.7\times10^6\,\mathrm{J\cdot m^{-3}\cdot K^{-1}}$. The outer surface of the sample was assumed to be opaque, black and insulated.

The temperature curves obtained for the two thermocouples were treated as numerical experiments to estimate the values of the parameters λ_{est}, ρc_{est} and T_1, using the E2 estimation method described previously. The time interval over which the estimation was performed was adjusted for each curve to obtain flat and

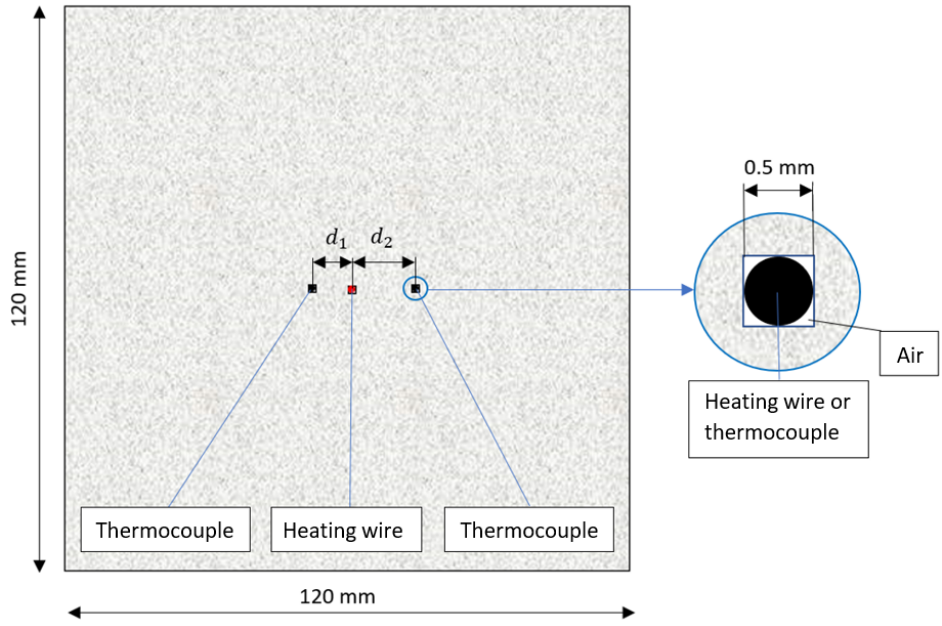

Figure 6: Diagram of the modeled system with $d_1 = 10\,\text{mm}$ and $d_2 = 15\,\text{mm}$.

zero-centered estimation residuals over this interval. The estimated value λ_{est} was then compared to the apparent conductivity calculated by:

$$\lambda = \lambda_{\text{c}} + \frac{16}{3}\,\frac{\sigma \overline{T}^3}{\beta} \tag{21}$$

Where λ_{c} is the phonic conductivity used in the COMSOL Multiphysics® simulation β is the extinction coefficient, and $\overline{T}$ is the average temperature of the measurement point as recommended by Gross et al. [8]. The estimated value ρc_{est} was also compared to the nominal value ρc. The analysis of all the results showed that there is no significant difference between the values estimated with $d = 10\,\text{mm}$ and those estimated with $d = 10\,\text{mm}$. Figure 7 shows the relative deviations between the values of apparent conductivity λ_{est} estimated from the temperature at 15 mm and the nominal values calculated by Equation (21) as a function of the Stark number defined by Viskanta [18] and Cintolesi et al. [19] and presented in Equation (22):

$$N = \frac{\beta \lambda_{\text{c}}}{4\sigma \overline{T}^3} \tag{22}$$

It is proportional to the ratio of the thermal conductivity λ to the radiative conductivity λ_{r}.

Figure 7a shows that in the case of the PHW method for the estimation error to be less than 2 % it is necessary that:

- $N > 0.1$ in the case of an absorbing and scattering material, see Figure 7a.
- $N > 2$ in the case of a purely scattering material, this limit value can be lower for materials of low thermal conductivity ($N > 0.8$ for $\lambda = 0.1\,\text{W} \cdot \text{m}^{-1} \cdot \text{K}^{-1}$ for example), see Figure 7b.

Figure 8 shows the relative deviations between the values of the volumetric heat capacity estimated from the 15 mm measurement and the nominal values as a function of the Stark number. It shows that for the estimation error to be less than 2 % it is necessary that $N > 0.5$ in the case of an absorbing and scattering material, see Figure 8a. In the case of a purely scattering material, the Stark number must be greater than 10 for the accuracy to be better than 5 %.

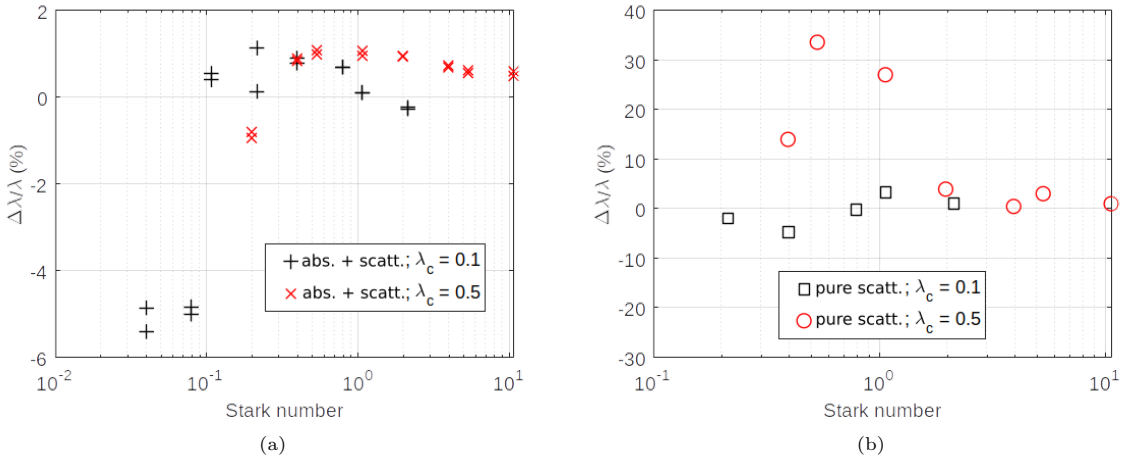

Figure 7: Relative deviation $\left(\frac{\Delta\lambda}{\lambda} = \frac{\lambda_{\text{est}} - \lambda_{\text{nom}}}{\lambda_{\text{nom}}}\right)$ between the apparent conductivity values (λ_{est}) estimated from the 15 mm PHW measurements and the nominal values ($\lambda_{\text{nom}} = \lambda_{\text{c}} + \lambda_{\text{r}}$) as a function of the Stark number in (a) the absorption-diffusion case and (b) the pure scattering case.

It should also be noted that the estimation time interval decreases when the extinction coefficient decreases and this is all the more so as the share of scattering is large. On the one hand the time required for radiation to be well taken into account by a conductive model with apparent thermal conductivity increases, and on the other hand, the increase of the apparent thermal conductivity when the extinction coefficient β decreases makes the assumption of the semi-infinite medium less valid. As an example, the estimation interval for the high density thermal insulating material varies from 0 s to 1000 s for $\beta = 10000$ at $T = 1000\,^{\circ}\text{C}$ to 80 s to 250 s for $\beta = 500$ at $T = 1500\,^{\circ}\text{C}$.

6. Results and discussion

6.1. Distance calibration

The main source of uncertainty in the estimation of the volumetric heat capacity is the uncertainty in the distance d between the heating wire and the thermocouple. The uncertainty on this distance is of the order of 0.5 mm given the brittleness of the materials in which the grooves are made. For a distance $d = 10$ mm, this leads to an uncertainty of 5 % on and an uncertainty of 10 % on ρc [3]. To reduce this uncertainty, we performed three parallel hot-wire experiments at 20 °C for each of the 3 SilPower® samples which specific heat at 20 °C was measured by differential scanning calorimetry using the Setaram μdSc$_3$ apparatus and we obtained : $c = 760\,\text{J}\cdot\text{kg}^{-1}\cdot\text{K}^{-1}$. The accuracy of the measurement is estimated at 2 %. These experimental curves were used to estimate the unknown parameters λ, d and R considering the known value of ρc.

The results are presented in Table 2. A very good reproducibility of the measurements is observed. It is also observed that the deviation between the estimated values and the nominal values can reach 5 %. Since the uncertainty on is mainly due to the error on d, the estimation error on ρc is reduced to the uncertainty on the reference value used to estimate the distances, i.e. about 2 %. The accuracy of the estimate is thus significantly improved.

6.2. Measurements on SilPower®

The estimated values of d_1 and d_2 were then used to estimate λ, ρc and R for the experiments performed between 200 °C to 1200 °C. Consistent with the results of the theoretical study, the values of λ and ρc estimated with the measured temperatures at distances d_1 and d_2 from the heating wire were almost identical. The average deviation observed for λ is 1.6 % and that for ρc is 2.1 %. The results obtained for λ and ρc are shown in Figures 9a and 9b respectively. The points correspond to the average of the 6 measurements performed (3 for each distance) and the bars represent the standard deviations of these groups of 6 points.

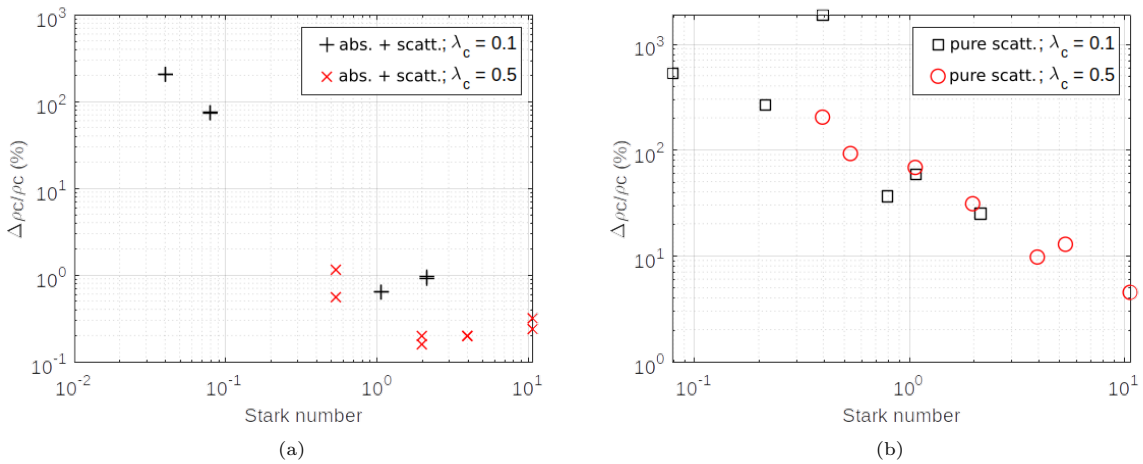

Figure 8: Relative deviation $\left(\frac{\Delta\rho c}{\rho c} = \frac{\rho c_{\text{est}} - \rho c_0}{\rho c_0}\right)$ between the volumetric heat capacities values estimated (ρc_{est}) from the 15 mm PHW measurements and the nominal values (ρc_0) as a function of the Stark number in (a) the absorption-diffusion case and (b) the pure scattering case.

Table 2: Estimated values of SilPower®thermal conductivity and heating wire-thermocouple distances at 20 °C.

	N°exp	$\boldsymbol{\lambda}$	$\mathbf{d_1}$	$\boldsymbol{\lambda}$	$\mathbf{d_2}$
		W m^{-1} K^{-1}	m	W m^{-1} K^{-1}	m
$\rho = 581$ kg m^{-3}	1	0.123	0.00999	0.121	0.01465
	2	0.124	0.10000	0.124	0.01467
	3	0.125	0.01001	0.125	0.01467
	Mean	0.124	0.01000	0.123	0.01466
$\rho = 741$ kg m^{-3}	1	0.169	0.00972	0.160	0.01417
	2	0.169	0.00972	0.160	0.01418
	3	0.168	0.00971	0.158	0.01478
	Mean	0.169	0.00972	0.159	0.01417
$\rho = 910$ kg m^{-3}	1	0.213	0.00938	0.211	0.01478
	2	0.217	0.00943	0.217	0.01491
	3	0.214	0.00946	0.214	0.1488
	Mean	0.215	0.00942	0.214	0.1485

The 21 standard deviations on ρc calculated each on 6 measurements were all less than 5 % with an average of 2.6 % which demonstrates the effectiveness of the distance calibration procedure.

The values of thermal conductivity increase as expected with temperature and with density. The values of the specific heat c are close for the three materials, which is logical given that they have the same composition. These values are also very close to those measured by Brückner for silica up to 600 °C [20] also shown in Figure 9. For temperatures above 800 °C, the difference between our values and those of Brückner increases with temperature, these differences will be explained later after the extinction coefficients of the different grades have been estimated.

Figure 10 shows the experimental and model curves from the estimated values as well as the estimation residuals ×10 for the SilPower®SG at 20 °C and at 1200 °C for the measurement at $d = 10$ mm. It can be seen that the residuals are perfectly flat and centered on the estimation interval [100 s; 800 s] which validates the model of an apparent thermal conductivity on this time domain. The estimation at 20 °C leads to perfectly flat residuals as early as 40 s while at 1200 °C we observe a divergence of the residuals up to 100 s. The estimated

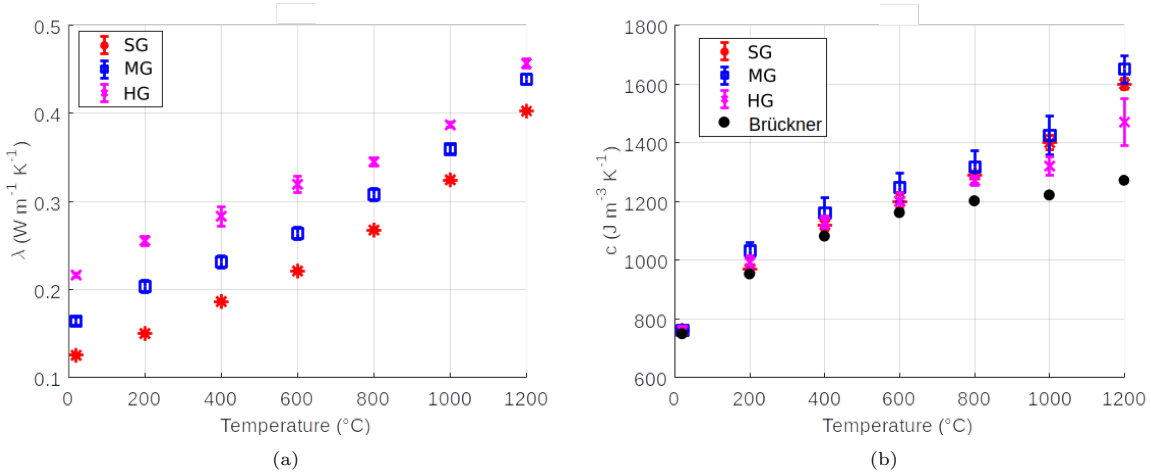

Figure 9: (a) - Estimated values of the apparent thermal conductivity ; (b) - Estimated values of the specific heat and values given by Brückner [20].

values of the temperature shift are $T_1 = -0.039\,°C$ at $20\,°C$ and $T_1 = 1.02\,°C$ at $1200\,°C$. The negative value at $20\,°C$ is due to the contact resistance in the absence of significant radiation at this temperature while the positive value at $1200\,°C$ is mainly due to the fact that the Rosseland model underestimates the radiation at short times and that the radiation, negligible at $20\,°C$, becomes significant at $1200\,°C$.

6.3. Estimation of the extinction coefficient

The following assumptions are made:

- The thermal conductivities of the solid and air in the porous medium evolve linearly with temperature.
- The radiation is represented by the Rosseland approximation with a constant extinction coefficient β.

The apparent thermal conductivity can therefore be written:

$$\lambda = a + bT + \frac{16n^2T^3}{3\beta} \tag{23}$$

For each material, we can then estimate the parameters a, b and β by minimizing the sum :

$$S = \sum_{j=1}^{J} \left[\lambda_{\text{exp}}\left(T_j\right) - \lambda_{\text{mod}}\left(T_j\right)\right]^2 \tag{24}$$

Where J is the number of temperatures for which the measurement of λ was performed. The standard deviation of the estimation error can then be evaluated by a Monte-Carlo type method. We perform the estimates on 10000 curves $\lambda_i(T)$ obtained by adding a random measurement noise to the curve $\lambda_{\text{exp}}(T)$ considering an uncertainty of $2\,\%$ on λ_{exp} :

$$\lambda_i\left(T_j\right) = \lambda_{\text{exp}}\left(T_j\right) + 0,05\left(0,5 - r_{i,j}\right) d\lambda_{\text{exp}} \tag{25}$$

Where r_{ij} is a random number between 0 and 1. The only uncertainty to be considered is that which varies from one measurement to the next. If there is a systematic error (e.g., in the length L of the wire), this error will be accounted for by the parameter a but will not affect the estimate of b and β. The value of $2\,\%$ is therefore certainly a bit overestimated.

The standard deviation over the 10000 estimates made of each of the parameters a, b and β is then calculated. The results are presented in Table 3 and the values of the different estimated conductivities are presented in Figure 11 for SilPower®SG and SilPower®HG. The following comments can be made:

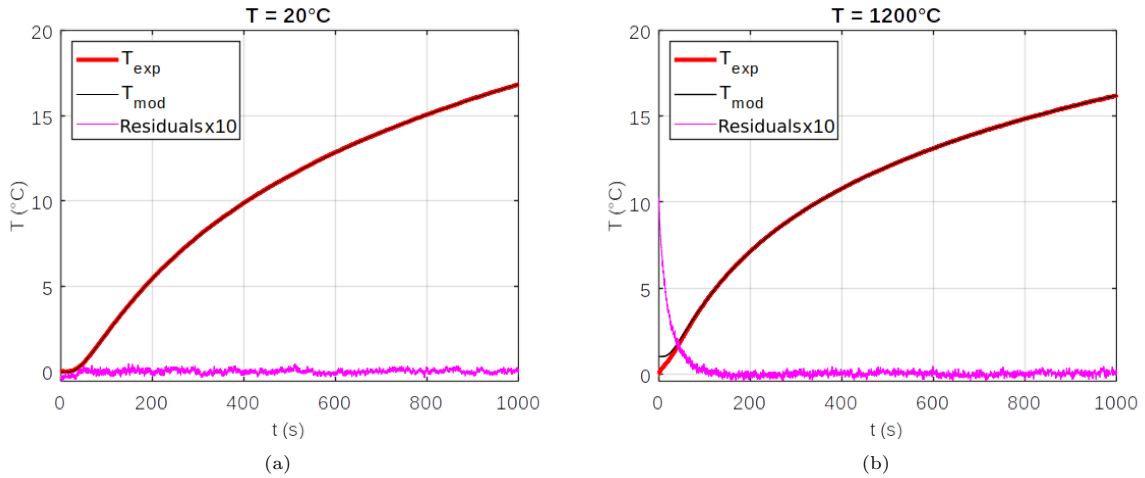

(a) (b)

Figure 10: Experimental curve and simulated curve with the values estimated between 100 s and 800 s both with estimation residuals ×10 for SilPower®SG (a) at 20 °C and (b) at 1200 °C for $d = 10$ mm.

- The extinction coefficient decreases very logically when the density decreases.
- The values of the apparent conductivity calculated with the estimated values of the parameters a, b and β coincide perfectly with the experimental values.
- It is often assumed that the thermal conductivity of the porous solid matrix is proportional to that of the solid [21]. Despite the high uncertainties, the ratios of the thermal conductivity of SilPower®at 1200 °C to its value at 20 °C (obtained for all three densities) are found to be very close (maximum deviation of 20 %) to that obtained for silica, of which the backbone of SilPower®is more than 99 % (see Table 3).
- The accuracy of the β estimate decreases when the value of β increases: this is explained by the fact that when β increases, the share of the radiative conductivity λ_r in the apparent conductivity λ decreases so the sensitivity of λ to β decreases.

Table 3: Estimated values of parameters a, b and β and their uncertainties.

	$\boldsymbol{\rho}$	$\boldsymbol{\beta}$	$\boldsymbol{\sigma_\beta}$	$\mathbf{a}$	$\sigma_\mathbf{a}$	$\mathbf{b}$	$\boldsymbol{\sigma_b}$	$\frac{\lambda_{c\ 1200\,°C}}{\lambda_{c\ 20\,°C}}$		
	kg m^{-3}	m^{-1}	%	W m^{-1} K^{-1}	%	W m^{-1} K^{-1}	%	thermal	SiO_2⋆	Air
SG	581 kg m^{-3}	6.92×10^3	7.8	9.19×10^{-2}	3.6	1.14×10^{-4}	6.8	2.4		
MG	741 kg m^{-3}	7.83×10^3	10	1.34×10^{-1}	3.0	1.19×10^{-4}	7.4	2.0	2.0	3.5
HG	910 kg m^{-3}	1.35×10^4	19	1.83×10^{-1}	2.6	1.31×10^{-4}	7.8	1.8		

⋆ from Combis et al. [22]

Estimates of the extinction coefficients β and thermal conductivities λ_c of the solid allow the calculation of the Stark number N for each grade and for each temperature. This then allows us to plot the relative differences between the estimated values ρc and those calculated from the Brückner values as a function of the Stark number N (see Figure 12). We plotted on the same graph the deviations between the values estimated from COMSOL Multiphysics® simulations for a scattering material ($k_s = 0.9999\beta$) and those from Brückner [20]. The deviations calculated from experiments and estimates follow the same trend and are close. SilPower® thus behaves as a highly scattering material towards radiation which is consistent with its properties: it is a highly reflective material (reflectivity greater than 95 % in the infrared [23]) and it contains a volume fraction of 60 % to 70 % of air (transparent) depending on the density.

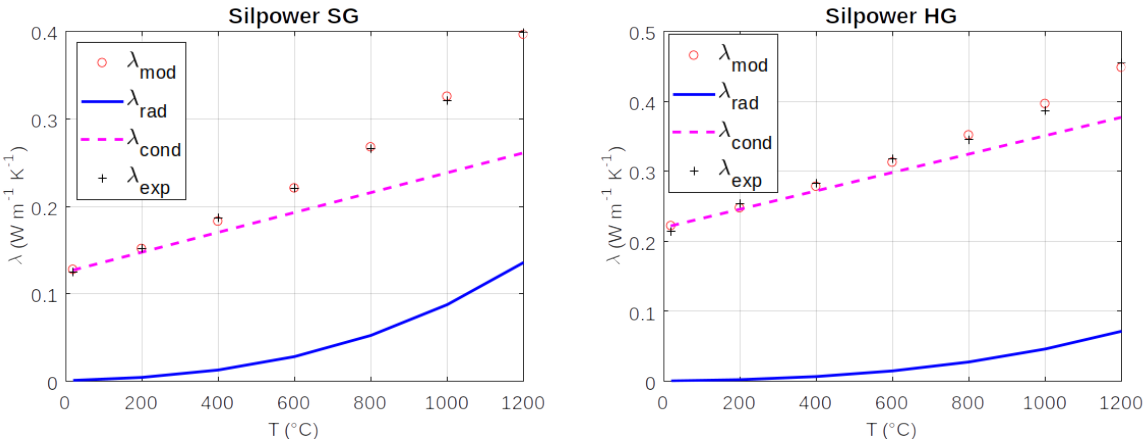

(a) SilPower® SG (b) SilPower® HG

Figure 11: Estimated values of the various conductivities for SilPower®SG and SilPower®HG.

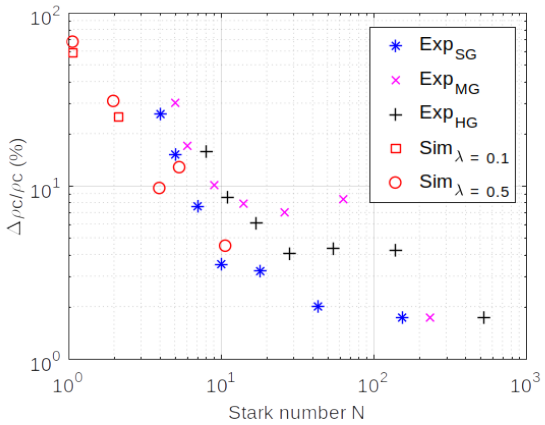

Figure 12: Relative deviation between the values of the specific heat estimated from experiments or simulations and those given by Brückner [20].

Finally, as an example, a COMSOL Multiphysics®simulation was performed with the estimated parameters for SilPower®SG at 1200 °C i.e. $\beta = 6920\,\mathrm{m}^{-1}$; $\lambda = \lambda_{\mathrm{est}} - \lambda_{\mathrm{r}}$ with $\lambda_{\mathrm{r}} = \frac{16}{3}\frac{\sigma \overline{T}^3}{\beta} = 0.140\,\mathrm{W}\cdot\mathrm{m}^{-1}\cdot\mathrm{K}^{-1}$ and $\lambda_{\mathrm{est}} = 0.267\,\mathrm{W}\cdot\mathrm{m}^{-1}\cdot\mathrm{K}^{-1}$; $\rho c = 8.63\times10^5\,\mathrm{J}\cdot\mathrm{m}^{-3}\cdot\mathrm{K}^{-1}$ and considering a highly scattering material ($k_{\mathrm{s}} = 0.9999\beta$). This simulation was then treated as an experimental curve to estimate λ and ρc. Figure 13a shows the curve simulated with COMSOL Multiphysics®the model curve plotted with the estimated parameters, and the estimation residuals. Figure 13b shows the experimental curve, the model curve plotted with the estimated parameters as well as the estimation residuals.

We can see that the residuals have globally the same shape and an amplitude of the same order of magnitude as those represented on Figure 9b, which confirms the very diffusive character of SilPower®. We note however that the residuals become zero only after 200 s for the simulation whereas they are null after 100 s for the experiment. This difference could be due to the approximations of the P1 model. It will therefore be necessary to develop a more accurate model if we want to represent the whole experimental curve in order to estimate for example the extinction or diffusion coefficient of the medium.

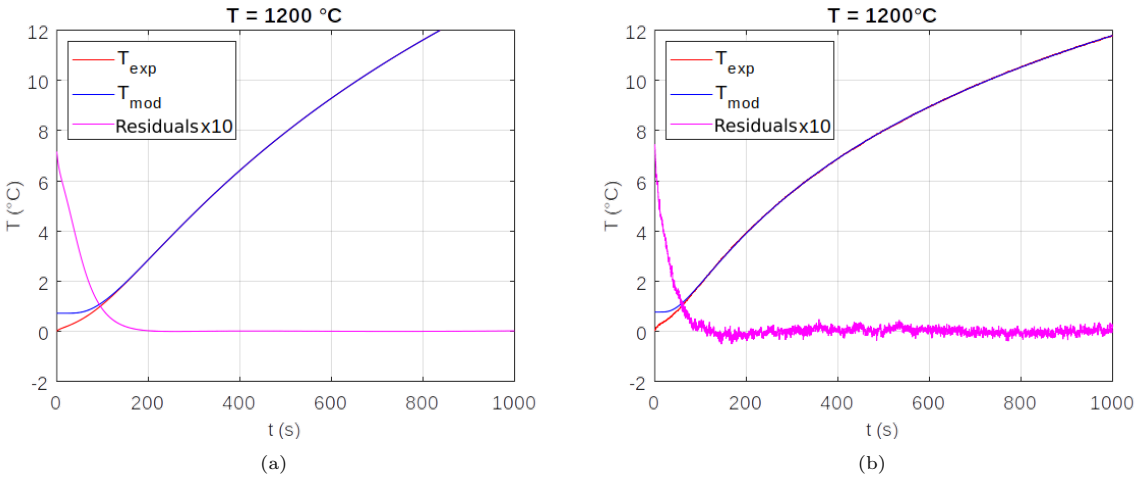

Figure 13: (a) - Simulated curve with COMSOL Multiphysics® and model curve ; (b) - Experimental curve and model curve.

Conclusion

The influence of the radiation heat transfer on the estimation of the thermal conductivity of a semi-transparent material by the parallel hot-wire method has been first investigated with COMSOL Multiphysics®using the coupled conduction-radiation module based on the P1 approximation for the radiation calculation. It was shown that the thermal conductivity may be estimated with an accuracy better than 2 % if the Stark number N (representing the ratio conduction/radiation) is :

- Greater than 0.1 for a purely absorbing or absorbing and scattering medium.
- Greater than 2 for a purely scattering medium.

It has also been shown that the classical estimation method based on the estimation of the three parameters (λ,ρc) leads to negative values of the thermal contact resistance R (it makes no physical sense) when radiation increases and creates an estimation bias. An new estimation method has been proposed to avoid this estimation bias.

A calibration process of the distance between the hot wire and the thermocouple has also been proposed and validated, enabling a more accurate estimation of the volume heat capacity. An experimental study carried out on three insulating materials with densities ranging from $581\,\mathrm{kg\cdot m^{-3}}$ to $910\,\mathrm{kg\cdot m^{-3}}$ and at temperatures ranging from 20 °C to 1200 °Cm^{-3} confirms the results of the theoretical study. A method enabling the estimation of the extinction coefficient from thermal conductivity measurements at various temperatures has been presented and successfully applied to the three tested materials.

References

[1] Yves Jannot and Alain Degiovanni. An improved model for the parallel hot wire: application to thermal conductivity measurement of low density insulating materials at high temperature. *International Journal of Thermal Sciences*, 142:379–391, 2019.

[2] Yves Jannot, Alain Degiovanni, Vincent Schick, and Johann Meulemans. Apparent thermal conductivity measurement of anisotropic insulating materials at high temperature by the parallel hot-wire method. *International Journal of Thermal Sciences*, 160:106672, 2021.

[3] ISO 18894-2:2007. Refractory Materials- Determination of thermal conductivity- Part 2: Hot-wire method (parallel) . Standard, International Organization for Standardization, Geneva, CH, March 2007.

[4] YZ Zhang, SX Cheng, JA Lee, and XS Ge. Simultaneous measurement of thermal conductivity and thermal diffusivity of solids by the parallel-wire method. *International journal of thermophysics*, 12(3): 577–584, 1991.

[5] G Grazzini, C Balocco, and U Lucia. Measuring thermal properties with the parallel wire method: a comparison of mathematical models. *International journal of heat and mass transfer*, 39(10):2009–2013, 1996.

[6] Wilson Santos and Rinaldo Jr. Numerical and experimental determination of minimum and maximum measuring times for the hot wire parallel technique. *Cerâmica*, 49, 03 2003. doi: 10.1590/S0366-69132003000100007.

[7] H-P Ebert and Jochen Fricke. Influence of radiative transport on hot-wire thermal conductivity measurements. *High Temperatures. High Pressures (Print)*, 30(6):655–669, 1998.

[8] Ulrich Gross et al. Radiation effects on transient hot-wire measurements in absorbing and emitting porous media. *International journal of heat and mass transfer*, 47(14-16):3279–3290, 2004.

[9] R Coquard, D Baillis, and D Quenard. Experimental and theoretical study of the hot-wire method applied to low-density thermal insulators. *International journal of heat and mass transfer*, 49(23-24): 4511–4524, 2006.

[10] Naouel Daouas, Ali Fguiri, and Med-Sassi Radhouani. Solution of a coupled inverse heat conduction–radiation problem for the study of radiation effects on the transient hot wire measurements. *Experimental thermal and fluid science*, 32(8):1766–1778, 2008.

[11] Frank R De Hoog, JH Knight, and AN Stokes. An improved method for numerical inversion of laplace transforms. *SIAM Journal on Scientific and Statistical Computing*, 3(3):357–366, 1982.

[12] Leonid Dombrovsky. P1 approximation of spherical harmonics method. In *Thermopedia*. Begel House Inc., 2011.

[13] R. E. Marshak. Note on the spherical harmonic method as applied to the milne problem for a sphere. *Phys. Rev.*, 71:443–446, Apr 1947. doi: 10.1103/PhysRev.71.443. URL `https://link.aps.org/doi/10.1103/PhysRev.71.443`.

[14] Yves Jannot and Alain Degiovanni. *Thermal properties measurement of materials*. John Wiley & Sons, 2018.

[15] Donald W Marquardt. An algorithm for least-squares estimation of nonlinear parameters. *Journal of the society for Industrial and Applied Mathematics*, 11(2):431–441, 1963.

[16] *Heat Transfer Module User's Guide*, 2020. URL `https://doc.comsol.com/5.6/doc/com.comsol.help.heat/HeatTransferModuleUsersGuide.pdf`. "Theory for Radiation in Participating Media, P1 Approximation Theory", pp. 268-271, COMSOL Multiphysics® v. 5.6.

[17] Yves Jannot, Alain Degiovanni, Vincent Schick, and Johann Meulemans. Thermal diffusivity measurement of insulating materials at high temperature with a four-layer (4l) method. *International Journal of Thermal Sciences*, 150:106230, 2020.

[18] RAYMOND Viskanta. Heat transfer by conduction and radiation in absorbing and scattering materials. *Journal of Heat Transfer*, 87(1):143–150, 1965.

[19] Carlo Cintolesi, Håkan Nilsson, Andrea Petronio, and Vincenzo Armenio. Numerical simulation of conjugate heat transfer and surface radiative heat transfer using the P 1 thermal radiation model: Parametric study in benchmark cases. *International Journal of Heat and Mass Transfer*, 107:956–971, April 2017. doi: 10.1016/j.ijheatmasstransfer.2016.11.006. URL `https://hal.archives-ouvertes.fr/hal-02070285`.

[20] Rolf Brueckner. Properties and structure of vitreous silica. i. *Journal of non-crystalline solids*, 5(2): 123–175, 1970.

[21] Matthias Rottmann, Thomas Beikircher, and Hans-Peter Ebert. Thermal conductivity of evacuated expanded perlite measured with guarded-hot-plate and transient-hot-wire method at temperatures between 295 k and 1073 k. *International Journal of Thermal Sciences*, 152:106338, 2020.

[22] Patrick Combis, Philippe Cormont, Laurent Gallais, David Hebert, Lucile Robin, and Jean-Luc Rullier. Evaluation of the fused silica thermal conductivity by comparing infrared thermometry measurements with two-dimensional simulations. *Applied Physics Letters*, 101(21):211908, 2012.

[23] Silpower®standard and high density. `https://www.quartz.saint-gobain.com/sites/imdf.quartz.com/files/silpower_leaflet_76014.pdf`. Accessed: 2021-12-14.